Live-Cell Imaging with Integrated Capacitive Sensor Arrays

J. K. Rosenstein¹, Y. Yin², K. Hu¹, S. Epstein², M. Wanunu², A. Adler³, and J. W. Larkin⁴

¹Brown University, Providence, RI, USA email: jacob_rosenstein@brown.edu

²Northeastern University, Boston, MA, USA ³Raytheon BBN, Cambridge, MA, USA ⁴Boston University, Boston, MA, USA

Abstract—Capacitive imaging is a near-field sensing technique that detects changes in the dielectric properties and geometry of materials above a microelectrode array. Taking advantage of modern integrated circuits, dense capacitive sensing arrays can now be created at the scales of single biological cells. These non-optical imaging arrays offer intriguing possibilities for cell culture monitoring, offering low cost, portability, single-cell resolution, a wide field of view, and co-integration with multiple electrochemical sensing and stimulation modes. Here we review state-of-the-art examples of capacitive imaging arrays and present new demonstrations of all-electrical imaging of growing bacterial cultures.

I. INTRODUCTION

Capacitance measurements are ubiquitous across applications ranging from MEMS accelerometers to touchscreen interfaces. Detecting changes in geometry or material composition using capacitance can be simple, reliable, label-free, inexpensive, and amenable to CMOS integration [1]–[4].

One growing but underexplored application of capacitance sensing is for monitoring and imaging of live cells. When capacitance sensing is implemented in a dense array, it can become a spatially-registered non-optical imaging modality. Capacitance sensing has been shown to make label-free measurements of cells' adhesion, proliferation, and growth in experimental settings. These demonstrations have included many different classes of cells, including but not limited to cardiac cells [5], epithelial cells [6], neural tissue [7], bacterial cells [8], fungal cells [9], and unicellular algae [10]. As microscale capacitance imaging arrays improve and mature, it seems clear that new biotechnology applications will emerge.

Here we review the fundamentals of capacitive imaging, discuss the state of the art in integrated CMOS capacitance imaging arrays, and present new demonstrations of all-electrical imaging of bacterial cultures.

II. ORIGINS OF CAPACITIVE IMAGES

Typically, each pixel in an image from a capacitive sensing array represents a single capacitance measurement, registered spatially within the array. The measured capacitance is a function of the local geometry and materials near one or more electrodes, and thus capacitance images can highlight spatial, temporal, and material differences. Depending on how the system is designed, individual measurements can correspond to the capacitance between each microelectrode and a common

reference, the total self-capacitance of each electrode, or the mutual capacitance between two planar electrodes (Fig. 1).

There are several options for measuring these capacitances. As for other imaging arrays, resolution and speed must be balanced with density, power, and frame rate. A lockin amplifier (Fig. 2a) is a classical and flexible option, if space and power are not a primary constraint. Switched-capacitor circuits (Fig. 2b) can be compact and efficient, and can be configured for either self-capacitance [11] or mutual capacitance measurements [12]. Ramp generators (Fig. 2c) can work well for larger interdigitated electrodes, but are generally not suitable for smaller microelectrodes and higher frequencies. Oscillator-based readout (Fig. 2d) can be very compact and sensitive, if process/voltage/temperature variation can be managed.

Coplanar microelectrodes generate three-dimensional fringe fields that extend vertically into the sample (Fig. 1c). Despite this complexity, some intuition can still hold from simpler parallel-plate capacitors. Signal contrast can come from differences in the effective local dielectric constant (ϵ) , effective area (A), or effective electrode separation (h). In idealized cases, coplanar electrodes can be mapped onto an equivalent parallel-plate geometry of $C = \epsilon A/h$ [13].

The fringing electric fields decay with distance, leading to a decrease in signal contrast for objects farther from the surface. In liquid media, at low frequencies ionic screening is dominant, leading to a double-layer capacitance that may be only tens of nanometers thick. At higher frequencies ($\gg 1 \text{MHz}$), Debye shielding is diminished, and the system behaves more like a bulk dielectric [11], [14]. In this regime, the effective sensing distance scales with the distance between two electrodes. Figure 1d plots a simulated example for point source electrodes on a surface separated by $20~\mu\text{m}$; beyond a depth of $20~\mu\text{m}$, the intensity of the electric field is reduced by more than 90%. The diminishing strength of the electric field is an indirect measure of the effective sensing depth, as objects farther from the surface contribute less to the observed capacitance.

Capacitive imaging can be performed with a background of either air or water. For cell cultures in aqueous media, the cell's proteins, lipids, and other organic molecules tend to reduce the effective dielectric constant relative to the surrounding water. Cells can also attach or adhere to the electrodes, affecting the double-layer capacitance [15].

III. LIVE-CELL IMAGING

Capacitive imaging and impedance imaging microarrays have been used with increasingly diverse cell cultures, ranging from microbes to mammalian cells.

In a system intended for cell viability screening in drug discovery, Wang and colleagues demonstrated impedance imaging of cardiomyocytes, integrated with cardiac pacing stimulation and extracellular potential recordings [5] (Fig. 5).

Abbott et al. developed a platform using impedance imaging of epithelial cells to evaluate confluence and adhesion during drug discovery. The same device also supports high voltage stimulation which clears the cells in a specified pattern, enabling *in situ* wound healing assays [6] (Fig. 6).

Widdershoven and colleagues imaged dynamic cell attachment and micromotion on a CMOS capacitance imaging chip with sub-micron electrode dimensions [11], [16] (Fig. 4). Lemay et al. have highlighted opportunities for reaching new electrochemical sensing regimes with nanoscale electrodes and radio frequency operation [14].

In our own work, we have previously shown capacitive imaging of *Bacillus subtilis* bacterial biofilms (Fig. 3e) [8], as well as unicellular green algae [10], [12] (Fig. 7).

In Figure 8, we present new measurements of *E. coli* microcolonies growing on a 131,072-pixel CMOS impedance imaging array. (This sensor chip is described in [17].) Over the course of two days, we were able to observe multiple phases of growth in the number of colonies near the sensor (Fig. 8c). Since the cells $(1-2 \, \mu \text{m})$ are smaller than the electrodes ($\approx 10 \, \mu \text{m}$) many of these colonies simply appear as a single pixel. Yet interestingly, the dielectric contrast of these single-pixel colonies also increased over time (Fig. 8c), which may correlate with the number of cells in the colony.

For larger cells or larger colonies, we can observe the same object on multiple pixels and more directly quantify their size and growth. Figure 9 shows an *E. coli* measurement in which larger colonies were observed. Using the same sensor [17] over a longer period of time, we were able to track the progression of bacterial colonies from their initial appearance at a single pixel as they grew to larger colonies with interesting morphologies occupying dozens or hundreds of pixels.

IV. DISCUSSION

One important consideration is that capacitive sensing arrays should be matched to the objects they are sensing. If possible, the electrode array pitch should be smaller than the smallest feature that one hopes to resolve. However, there is a tradeoff between better lateral resolution (smaller electrodes) and better sensing depth (larger electrodes). To some degree there are strategies to improve this tradeoff space; for example, by using multiple capacitance sensing patterns [18], computationally generating composite images with higher resolution [12] (Fig. 7), or by operating at higher frequencies to limit screening effects [14].

Similar to other imaging techniques, there are also interesting considerations around the projection of 3-D objects onto

2-D images. Capacitance imaging can also be used for 3-D tomography [19], in which a 3-D map of the sample is solved as an inverse problem from a series of capacitance measurements. Electrical capacitance tomography (ECT) can be computationally challenging, but it has been demonstrated at larger scales [20], and if appropriate microelectrode arrays and algorithms are developed, ECT has the potential to be extended down to microscale tissues, cultures, and single cells [8].

Platforms for cellular capacitance imaging can be low cost (even single-use and disposable), physically small, and portable, with no optics and no moving parts. Capacitive sensing can be co-integrated with other electrochemical sensing and stimulation modes, and it can detect, quantify, and image a wide range of cell types, without dyes or labels.

Capacitance imaging may not always match the resolution of the most expensive optical microscopes, but its low cost, portability, and versatility offer many exciting possibilities for future applications incorporating live cell imaging.

ACKNOWLEDGMENT

This work was supported in part by the National Science Foundation under Grant No. 2027108, by a grant from the Defense Advanced Research Projects Agency (DARPA), and by a Brown University Hazeltine Innovation Award.

REFERENCES

- [1] R. Puers, Sensors and Actuators A: Physical, 1993.
- [2] X. Hu and W. Yang, Sensor Review, 2010.
- [3] V. Tsouti, C. Boutopoulos et al., Biosensors and Bioelectronics, 2011.
- [4] S. Forouhi, R. Dehghani et al., Sensors and Actuators A: Physical, 2019.
- [5] J. S. Park, M. K. Aziz et al., IEEE transactions on biomedical circuits and systems, 2017.
- [6] J. Abbott, A. Mukherjee et al., Lab on a Chip, 2022.
- [7] V. Viswam, R. Bounik et al., IEEE transactions on biomedical circuits and systems, 2018.
- [8] K. Hu, J. Incandela et al., in 2022 IEEE Custom Integrated Circuits Conference (CICC). IEEE, 2022.
- [9] A. Romani, N. Manaresi et al., in IEEE International Solid-State Circuits Conference. IEEE, 2004.
- [10] C. E. Arcadia, K. Hu et al., in 2021 IEEE International Symposium on Circuits and Systems (ISCAS). IEEE, 2021.
- [11] C. Laborde, F. Pittino et al., Nature nanotechnology, 2015.
- [12] K. Hu, J. Ho et al., IEEE Transactions on Biomedical Circuits and Systems, 2022.
- [13] A. V. Mamishev, K. Sundara-Rajan et al., Proceedings of the IEEE, 2004.
- [14] M. Saghafi, S. Chinnathambi et al., Current Opinion in Colloid & Interface Science, 2022.
- [15] S. B. Prakash and P. Abshire, Biosensors and Bioelectronics, 2008.
- [16] F. Widdershoven, A. Cossettini et al., IEEE transactions on biomedical circuits and systems, 2018.
- [17] K. Hu, C. E. Arcadia et al., IEEE Solid-State Circuits Letters, 2021.
- [18] K. Hu, C. E. Arcadia et al., in IEEE Sensors Conference, 2021.
- [19] W. Yang and L. Peng, Measurement science and technology, 2002.
- [20] Z. Ye, R. Banasiak et al., Insight-Non-Destructive Testing and Condition Monitoring, 2013.
- [21] P. S. Joshi, K. Hu et al., in 2022 IEEE Biomedical Circuits and Systems Conference (BioCAS). IEEE, 2022.
- [22] J. Št'astný, *Fottea*, 2010.

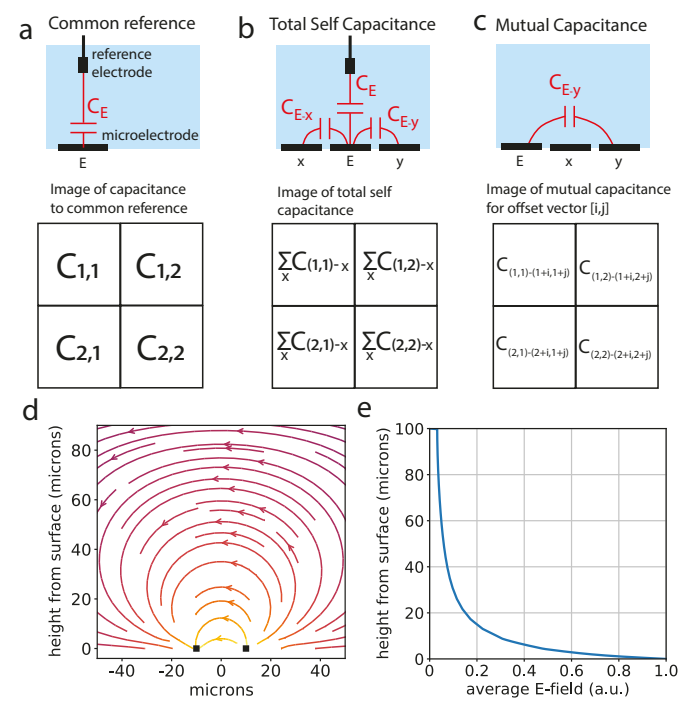


Fig. 1. Capacitance sensing and image formation. (a) In one configuration, each microelectrode is measured relative to a common reference. In water at lower frequencies when Debye screening is dominant, this would often be the bulk electrolyte potential. (b) In another arrangement, the total self-capacitance is measured, which includes fringing fields to all other nearby pixels. (c) Each measurement can also represent the mutual capacitance between pairs of offset electrodes, where the positions of both electrodes shift through the array to form an image. (d) A simulated example of the fringe fields coupling two electrodes separated by 20 microns. (e) The average field intensity from panel c, which decays with distance from the surface. Electric field intensity is an indirect measure of the sensitivity to objects at that distance.

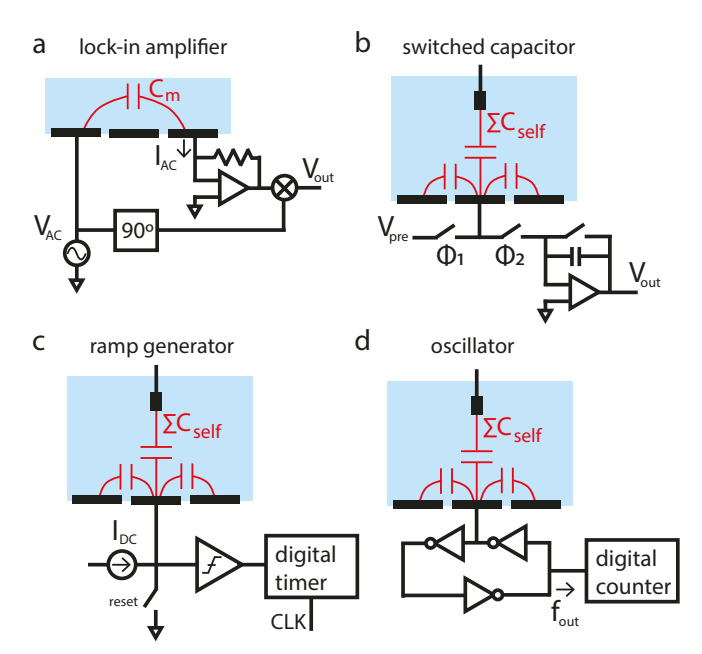


Fig. 2. Capacitance sensing circuits. (a) Lock-in amplifier. (b) Switched-capacitor amplifier or integrator. (c) Ramp generator and digital timer. (d) Oscillator based capacitance measurement.

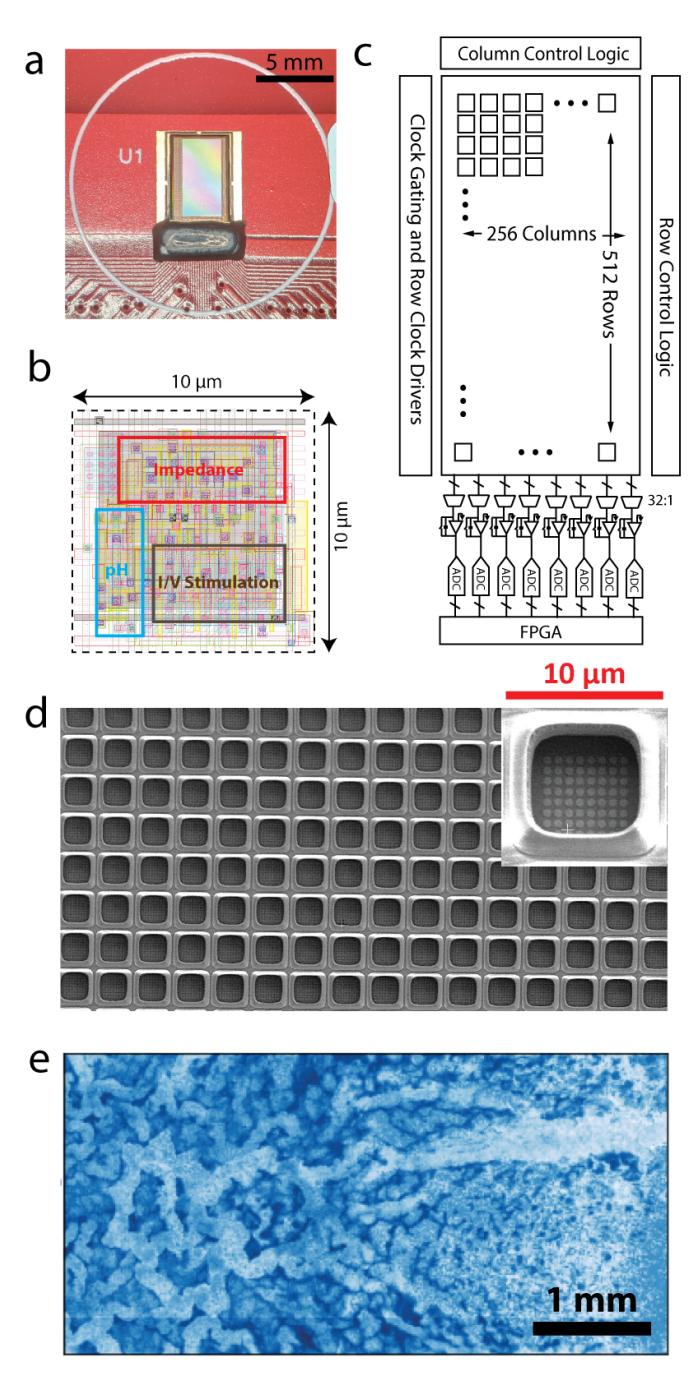


Fig. 3. Design of a 512×256 CMOS microelectrode array [8]. (a) Photograph of a CMOS electrochemical sensor array. (b) Beneath the microelectrode in each pixel, there are addressable circuits which can measure impedance, capacitance, or pH, or provide electrical stimulation [21]. (c) The overall array is structured with row-column addressing, and columns are multiplexed into eight parallel readout paths. (d) A scanning electron microscope image of a portion of the array, after the aluminum top metal has been chemically etched away. (e) An example capacitance image of a *Bacillus subtilis* biofilm on the sensor array. The capacitance image is able to resolve many complex spatial features within the biofilm. © 2022 IEEE. Reprinted, with permission, from Hu et al. [8]

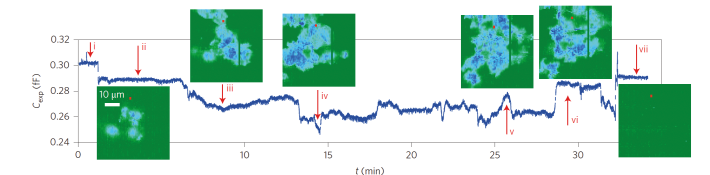


Fig. 4. Adapted from Laborde et al. [11]. Time-lapse capacitance imaging of MCF-7 breast cancer cells. The time series is the capacitance of a single pixel, and the inset images are impedance images at several time points. i, PBS washing of the sensor; ii, introduction of cells; iii, cell attachment; iv-v, fluctuations due to changes in attachment of cells to the electrode surface; vi, spontaneous detachment and reattachment; vii, washing. Image reproduced with permission from Springer Nature.

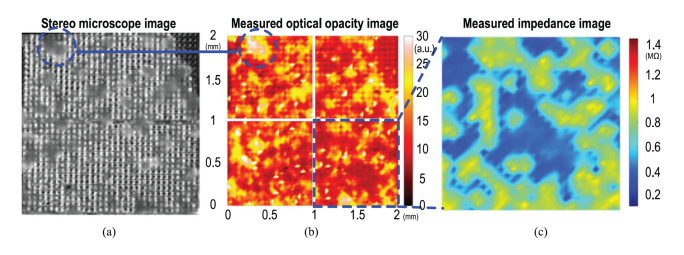


Fig. 5. Adapted from Park et al. [5]. Rat cardiomyocyte cells cultured on a 1024-pixel multimodal CMOS sensor array. (a) Optical microscope image of the cells on the electrode array. (b) Optical opacity measurement. (c) Impedance image from a subset of the array. © 2017 IEEE. Reprinted, with permission, from [5].

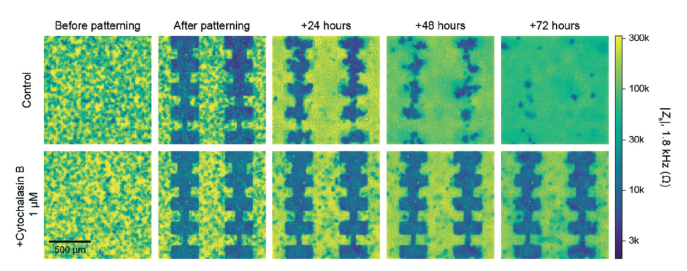


Fig. 6. Adapted from Abbott et al. [6]. A wound healing assay was implemented on a CMOS microelectrode array, in which epithelial cells were spatially removed and allowed to grow back. A control sample recovered in 72 hours (top row), but a sample treated with a motility inhibitor drug (bottom row) was much slower to recover. Image © The Royal Society of Chemistry 2022, CC BY-NC 3.0.

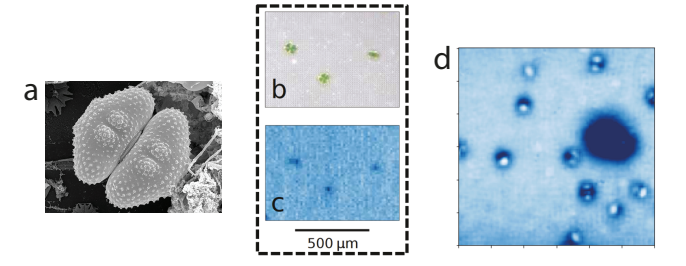


Fig. 7. Adapted from Arcadia et al. [10] and Hu et al. [12]. Algae super-resolution impedance imaging. (a) A reference electron microscope image of a *Cosmarium* green microalgae cell, with its characteristic bi-lobal structure. Image by J. Šťastný [22]. (b) Optical microscope images of *Cosmarium* cells on a CMOS sensor array. (c) Capacitance images of the cells from the CMOS sensor array [10]. The data is clear enough to count the algae cells, but not to see any fine structure. (d) Super-resolution impedance image of *Cosmarium* on a CMOS sensor array [12], constructed from multiple variations of mutual capacitance images of the same scene. The bilobal structure of the microalgae cells are clearly evident. © 2021 IEEE. Panels b-c reprinted, with permission, from Arcadia et al. [10]. Panel d is from Hu et al. [12].

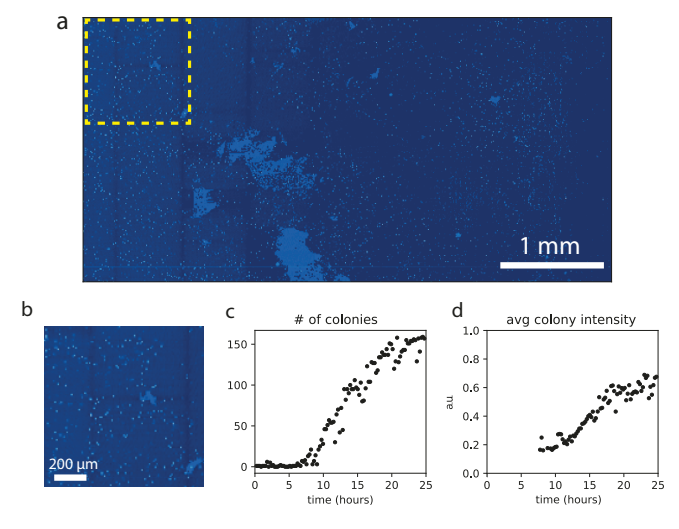


Fig. 8. Time-lapse capacitance imaging of E. coli colony growth. (a) Whole 512×256 image at the end of 2 days of growth, using the CMOS sensor from [17]. (b) Zoom in to the highlighted area. (c) Number of colonies over time, for the highlighted area. (d) Average impedance contrast over time, for the highlighted area. Since most of these colonies have sub-pixel dimensions, the intensity may correlate with colony size.

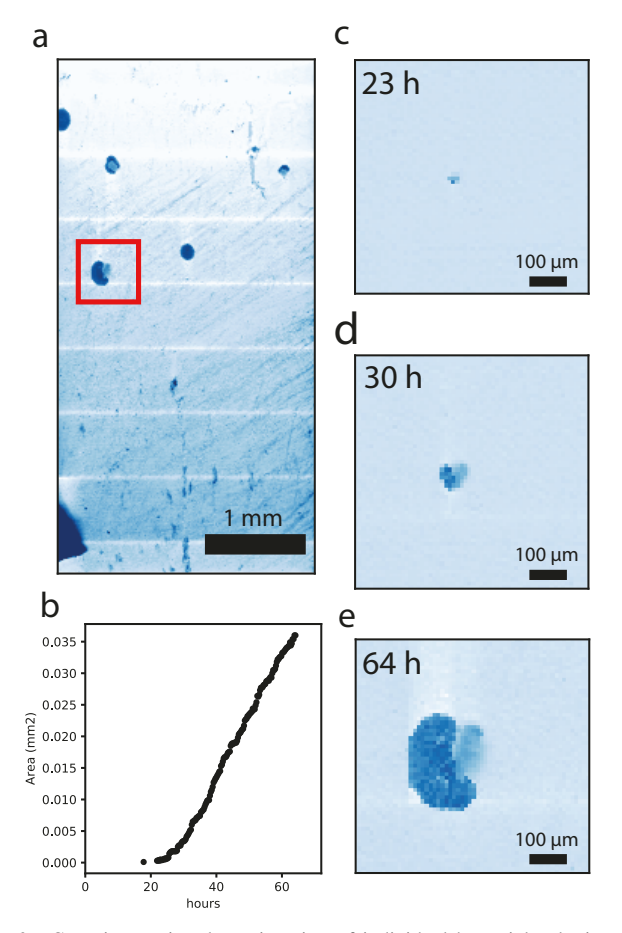


Fig. 9. Capacitance time-lapse imaging of individual bacterial colonies. (a) 512×256 impedance image of an *E. coli* culture after 2.5 days of growth. (b) The approximate area of one colony (red box), quantified over time. (c,d,e) Images of the same colony after 23, 30, and 64 hours.